RESEARCH ARTICLE
SPACE PHYSICS

Earth and Planetary Physics
9: 491–499, 2025
doi: 10.26464/epp2025062

Technical characteristics of Macau Science Satellite-1A

Yan Li[1], Yong Zhang[1], TianYu Zhang[1], ShiGeng Yuan[2], Wen Su[1], JingShan Sun[1], Fei Feng[1*], BingJun Cheng[3], Yi Jiang[4], PengFei Liu[4], GuiHong Xiao[1], QingMei Fan[2], ChunYu Yu[2], Ming Wang[2], Qi Xiao[2], and ChuNan Miao[1]

[1]DFH Satellite Co. Ltd., Beijing 100094, China;

[2]Beijing Institute of Spacecraft System Engineering, China Academy of Space Technology, Beijing 100094, China;

[3]National Space Science Center, Chinese Academy of Sciences, Beijing 100190, China;

[4]Macau Institute of Space Technology and Application, Macau University of Science and Technology, Macao 999078, China

Key Points:

- The Macau Science Satellite-1A (MSS-1A) has achieved measurement accuracy for both the three-component magnetic field and total magnetic field intensity that is consistent with ground test results.
- The MSS-1A satellite has achieved a number of major breakthroughs in magnetic measurement technology.
- The MSS-1A serves as a valuable reference for satellite design, data processing, and international cooperation.

Citation: Li, Y., Zhang, Y., Zhang, T. Y., Yuan, S. G., Su, W., Sun, J. S., Feng, F., Cheng, B. J., Jiang, Y., ... and Miao, C. N. (2025). Technical characteristics of Macau Science Satellite-1A. *Earth Planet. Phys.*, *9*(3), 491–499. http://doi.org/10.26464/epp2025062

Abstract: The Macau Science Satellite-1 (MSS-1) is the first space science satellite jointly developed on the Chinese mainland and in Macau. It comprises two satellites, named MSS-1A and MSS-1B, and holds considerable importance in China's space exploration endeavors. Among these, MSS-1A is the world's first high-precision scientific satellite dedicated to exploring the geomagnetic field and space environment at low latitudes. Equipped with two high-precision vector magnetometers and one scalar magnetometer, which are integrally installed on a highly stable nonmagnetic optical bench, the MSS-1A enables simultaneous high-precision measurements of both the Earth's vector magnetic field and its scalar components. Its design integrates several state-of-the-art technologies, including arc-second-level thermal stability control, nonmagnetic thermal control for the optical bench, and ultra-high magnetic cleanliness control. These innovations effectively minimize magnetic interference originating from the satellite itself, thereby substantially improving the precision of geomagnetic field measurements and establishing a robust technical foundation for future magnetic survey satellite constellations.

Keywords: Macau Science Satellite-1; system design; geomagnetic field observation; optical bench; magnetic cleanliness control

1. Introduction

The geomagnetic field is one of Earth's critical physical fields, exerting profound influences on geophysical processes, biological activities, and the space environment. However, the characteristics of Earth's magnetic field variations in numerous low-latitude regions, particularly in the South Atlantic Anomaly (SAA), remain shrouded in mystery. To address this research gap, the Government of the Macau Special Administrative Region (SAR) and the China National Space Administration (CNSA) jointly launched the Macau Science Satellite-1 (MSS-1) project. This initiative aims to advance cutting-edge research in Earth sciences through high-precision geomagnetic field and space environment exploration (e.g., Zhang K, 2023).

As a major scientific endeavor to enhance Macao's technological innovation capabilities and strengthen collaboration between China's mainland and Macao, the MSS-1 project was officially inaugurated on October 9, 2019, coinciding with the 20th anniversary of Macao's return to China. After 4 years of development, the satellite was successfully launched into orbit on May 21, 2023. Operating at an altitude of 450 km with an inclination of 41° and a design lifetime of 5 years, the satellite has undergone rigorous in-flight testing and evaluation. All functions and performance metrics fully meet the mission requirements, with the measurement accuracy of the three-component magnetic field and total magnetic field intensity being consistent with the ground test results. Notably, it has achieved the first-ever rapid traversal of Earth's east–west magnetic field across all 24 local time zones and has captured the most densely sampled magnetic field data over the SAA. These breakthroughs position the satellite as a critical data source for establishing and updating high-precision global magnetic field models.

2. Overview of Developments

The mission objectives of geomagnetic survey satellites have evolved from single-satellite, single-point detection to multi-satellite, collaborative global observations, shifting the focus from

First author: Y. Li, 13693569168@139.com
Correspondence to: F. Feng, 153682945@qq.com
Received 07 FEB 2025; Accepted 15 APR 2025.
First Published online 29 APR 2025.

probing Earth's main magnetic field to studying geospace physics in the magnetosphere–magnetotail regions (e.g., Friis-Christensen et al., 2006; Feng Y et al., 2010; Liu JH et al., 2024). Early developments in geomagnetic satellites progressed rapidly such that within only a decade of the launch of the first satellite, measurement accuracy had already reached the order of 10 nT. However, because of limitations such as orbit positioning accuracy, absolute timing accuracy, and digitization accuracy, the output precision of geomagnetic field data was still lagging substantially behind instrumental measurement capabilities. With technological advances, subsequent satellites have achieved high-precision magnetic measurements while also integrating instruments for comprehensive exploration of nonmagnetic fields, such as gravitational fields and the ionosphere, driving progress in geophysics. A summary of representative geomagnetic survey satellites from domestic and international programs is provided in Table 1.

3. Satellite Mission

The MSS-1 constellation comprises two satellites, MSS-1A and MSS-1B, designed for collaborative high-precision exploration of Earth's geomagnetic field and low-latitude space environment. The MSS-1A is the primary satellite, jointly developed on the Chinese mainland and in Macao. It is the world's first scientific satellite dedicated to high-resolution geomagnetic field measurements at low latitudes. It focuses on mapping magnetic anomaly areas (e.g., the SAA), studying space weather interactions, and advancing deep Earth and ocean magnetic field modeling (Zhang K, 2021).

The second satellite, the MSS-1B, is equipped with a variety of scientific payloads, such as solar X-ray detectors, medium-energy particle detectors, and laser retroreflectors. Its primary missions focus on the observation of solar activity and the exploration of Earth's radiation belts. This article focuses on presenting the key characteristics and primary mission details of the MSS-1A satellite.

3.1 Mission Requirement

The MSS-1A is the world's first scientific exploration satellite dedicated to monitoring the geomagnetic field and space environment in the SAA. By obtaining high-precision data on the Earth's main magnetic field and lithospheric magnetic field in the SAA, as well as information on the energy particle and energy spectrum distribution in the inner radiation belt, it is expected to achieve internationally outstanding research results in fundamental and applied fields, such as lithospheric magnetic field distribution, the geodynamo, geomagnetic polarity reversal, space weather forecasting, geomagnetic navigation, and spacecraft operational safety in space. The primary physical quantities detected by the satellite are the Earth's magnetic field and energetic particles.

3.2 Satellite System Design

The MSS-1A satellite utilizes the China Academy of Space Technology 2000 (CAST2000) satellite platform, which consists of the payload and a platform service system. The total launch mass of the satellite is approximately 573 kg. Compared with an orbital altitude of 500 km, an altitude of 450 km enhances the satellite's detection capability for crustal field intensity (improved by 36%), substantially improving the detection sensitivity and accuracy of geomagnetic field models. A circular orbit with an inclination of 41° achieves full coverage of magnetic latitudes up to 30° (with some key areas reaching up to 50°), complete coverage of local time in 52 days, and a total observation time over the SAA of greater than 5% of the satellite's total lifespan. Therefore, considering the enhancement of magnetic field detection sensitivity, coverage of key areas, and local time coverage, a circular orbit with an altitude of 450 km and an inclination of 41° was chosen as the mission orbit for the MSS-1A satellite.

The platform service system is composed of subsystems, including structure and mechanism, attitude and orbit control, thermal control, telemetry and command, onboard management, and power. A compartmentalized configuration was adopted for the satellite, consisting of a platform cabin, a conical section, and a body-mounted solar array. All onboard electronic equipment is housed within the platform cabin, whereas the conical section provides structural support for the deployable boom and the body-mounted solar array. In consideration of the magnetic control requirements, the satellite uses pure thruster-based attitude control instead of magnetic torquers for momentum management.

The payload consists of scientific instruments, a high-precision optical bench, and a data transmission subsystem. The scientific instruments include the Vector Field Magnetometer (VFM) and the micro Advanced Stellar Compass (ASC), both developed by the Technical University of Denmark; the Coupled Dark State Magnetometer (CDSM), provided by the Austrian Academy of Sciences; and the Fluxgate Magnetometer (FGM), Energetic Electron Spectrometer (EES), and laser retro-reflector, developed by domestic institutions (see Figure 1).

Table 1. Overview of typical magnetic field survey satellites.[a]

Satellite name	Country	Time	Altitude (km)	Inclination (°)	Main payload	Optical bench availability	Overall measurement accuracy (nT)
MAGSAT	USA	1979	~350–550	96.7	Vector/scalar	No	6
Ørsted	Denmark	1999	~650–860	96.5	Vector/scalar	No	4
CHAMP	German	2000	456	87.3	Vector/scalar	No	2
SAC-C	Argentina	2001	~698–705	97	Scalar		2
Swarm	ESA	2013	~450–530	88	Vector/scalar	Yes	0.5
CSES	China	2018	507	97.4	Vector/scalar	No	1

[a]MAGSAT, Magnetic Field Satellite; CHAMP, Challenging Minisatellite Payload; SAC-C, Satélite de Aplicaciones Científicas-C; ESA, European Space Agency; CSES, China Seismo-Electromagnetic Satellite.

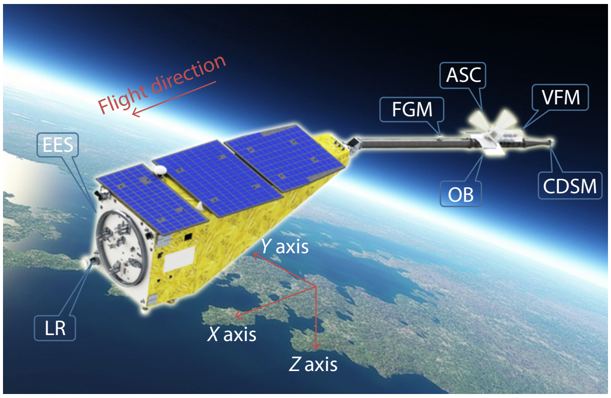

Figure 1. The MSS-1A in flight. Key technical parameters of the satellite are listed in Table 2. EES, Energetic Electron Spectrometer; LR, laser retro-reflector; FGM, Fluxgate Magnetometer; ASC, micro Advanced Stellar Compass; VFM, Vector Field Magnetometer; CDSM, Coupled Dark State Magnetometer; OB, optical bench.

The VFM enables highly accurate three-component magnetic field measurements, whereas the CDSM provides precise total magnetic field intensity data (e.g., Cheng BJ et al., 2018). Together, these instruments achieve state-of-the-art performance in detecting magnetic field gradients, particularly in the east–west direction, thereby contributing to the establishment of high-precision global geomagnetic models. The ASC serves as an attitude sensor for the optical bench, enabling the determination of the three-axis orientation of the satellite payload frame relative to an inertial reference frame. The EES onboard the MSS-1A is a sophisticated scientific instrument designed to measure high-energy electrons in the Earth's inner radiation belt. Additionally, the satellite is equipped with a laser retroreflector to support precise orbit determination, which enhances the reliability and accuracy of the collected data. The VFM and the ASC are rigidly mounted on a high-precision optical bench with in-flight thermal deformation better than 1 arc second. This vector magnetic field measurement assembly, along with the CDSM, is installed on a high-stiffness, nonmagnetic boom approximately 4.5 m long. This design ensures the precision and stability of the spatial vector relationship and reduces the interference of the satellite itself on the magnetic field measurements.

Table 2. Main parameters of the MSS-1A.

No.	Instrument	Parameters
1	Coupled Dark State Magnetometer (CDSM)	Accuracy: Better than 0.3 nT Measurement range: 10,000–100,000 nT
2	Vector Field Magnetomotor (VFM)	Accuracy: Better than 0.5 nT Measurement range: ±65,000 nT Noise (RMS): ≤0.03 nT (0.1–15 Hz)
3	Micro Advanced Stellar Compass (ASC)	Pointing precision: 3-axis ≤ 1″ (1σ)
4	Fluxgate Magnetometer (FGM)	Frequency range: DC ~25 Hz Accuracy: Better than 1.0 nT Resolution: Better than 0.01 nT Measurement range: ±65,000 nT
5	Energy Electron Spectrometer (EES)	Measurement range: ~50 keV–2 MeV Energy resolution: Better than 10% Field of view: 180° × 30° Channel: 5 exponential distribution channels; 128 linear distribution channels
7	Optical Bench (OB)	In-flight deformation better than 1″
8	Data transmission	Band: X band Rate: 30 Mbps Data storage: ≥128 Gbit
11	Attitude control	Method: Rolling traction Pointing precision: 3-axis ≤ 0.1° (3σ) Measurement precision: 3-axis ≤ 0.03° (3σ) Stability: 0.001 (°/s) (3σ)
12	Telemetry and telecommand	Method: USB Rate: Uplink 2000 bps; downlink 16,384 bps
13	Magnetic cleanliness	Magnetic field perturbation uncertainty at CDSM position: Better than 0.2 nT
15	Life	>5 years

3.3 Rolling Traction Design

The attitude control uses a three-axis stabilization plus roll control method, with the capability to automatically adjust the roll angle by ±15° and ±25° based on the β angle. For the first time, an autonomous rolling traction attitude control mode based on the β angle has been proposed. Specifically, the satellite rolls by a specific angle along the *X*-axis of the orbital coordinate system. This innovation addresses the issue of poor spatial distribution of the *Y*-direction magnetic field in low-inclination orbits and improves the accuracy of in-flight magnetic field measurements. By implementing the rolling traction mode, the satellite's magnetic field projection in the *Y*-axis direction has been substantially improved, expanding from a narrow-band small area to nearly half of a "celestial sphere" surface that can cover the zero point (see Figure 2). This mode greatly enhances the data accuracy control capability for in-flight calibration of the vector magnetic field, allowing the calibration accuracy to be controlled at the level of 0.03 nT. In addition, it improves the satellite's energy supply and improves its thermal control boundary conditions.

4. Magnetic Measurement System

The same vector–scalar combined observation instruments as the Swarm satellites have been adopted for the MSS-1A satellite. The scalar magnetometer is used as the reference to calibrate the vector magnetometer (e.g., Ness et al., 1971; Meng LF et al., 2024). Scalar magnetometers based on quantum transition effects and spherical fluxgate vector magnetometers are used to jointly calibrate the intensity and direction information of the magnetic field in orbit, obtaining precise vector magnetic field data in the sensor frame (see Figure 3). When combined with attitude data from the star trackers on the high-precision optical bench, the magnetic field in the magnetic sensor coordinate system is transformed into the Earth's spatial coordinate system.

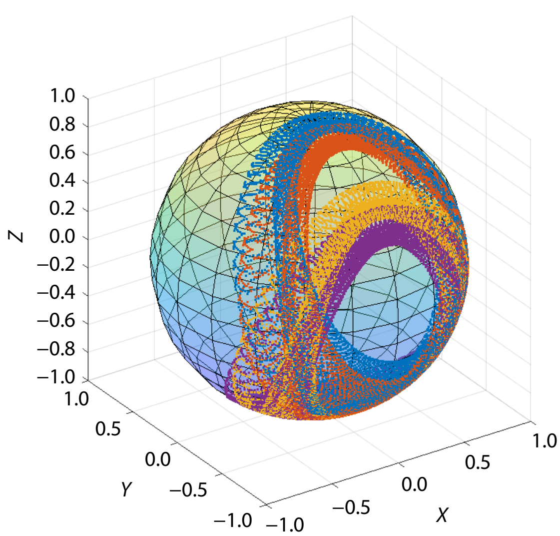

Figure 2. Celestial sphere coverage by the rolling traction mode.

4.1 Measurement Accuracy Analysis

In conjunction with the acquisition, calibration, and processing of high-precision magnetic field data, the full-chain accuracy for the high-precision magnetic field detection mission of the MSS-1A satellite has been decomposed, as shown in Figure 4.

In Figure 4, the green arrows represent the high-precision magnetic field data information flow on the satellite, the blue arrows indicate the ground data processing information flow, the purple sections denote the actual data products, the light blue sections represent the data processing operations, and the light red capsule-shaped patterns signify the accuracy introduced at each stage. Through categorization, the accuracy in magnetic field measurement can be divided into five parts according to the accuracy propagation system of magnetic field measurement:

- Original measurement accuracy of the magnetic field in the sensor coordinate system (E1–E3);
- Transformation accuracy from the sensor coordinate system to the Earth coordinate system (E4–E7);
- Satellite magnetic disturbance accuracy (E8);
- Other accuracy introduced during ground processing (E9).

By controlling various accuracy sources throughout the entire development process, the satellite system ultimately achieved a magnetic field measurement accuracy of better than 0.5 nT.

4.2 Optical Bench Design

To ensure the stability of the transfer matrix between the VFM and ASC under various operational conditions, the high-precision magnetic field measurement optical bench plays a crucial role (e.g., Friis-Christensen et al., 2006), as shown in Figure 5. There-

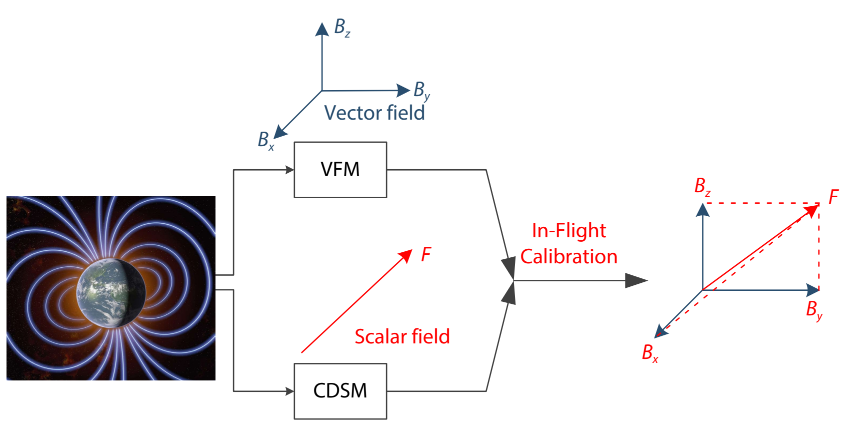

Figure 3. Observation system diagram. VFM, Vector Field Magnetometor; CDSM, Coupled Dark State Magnetometer.

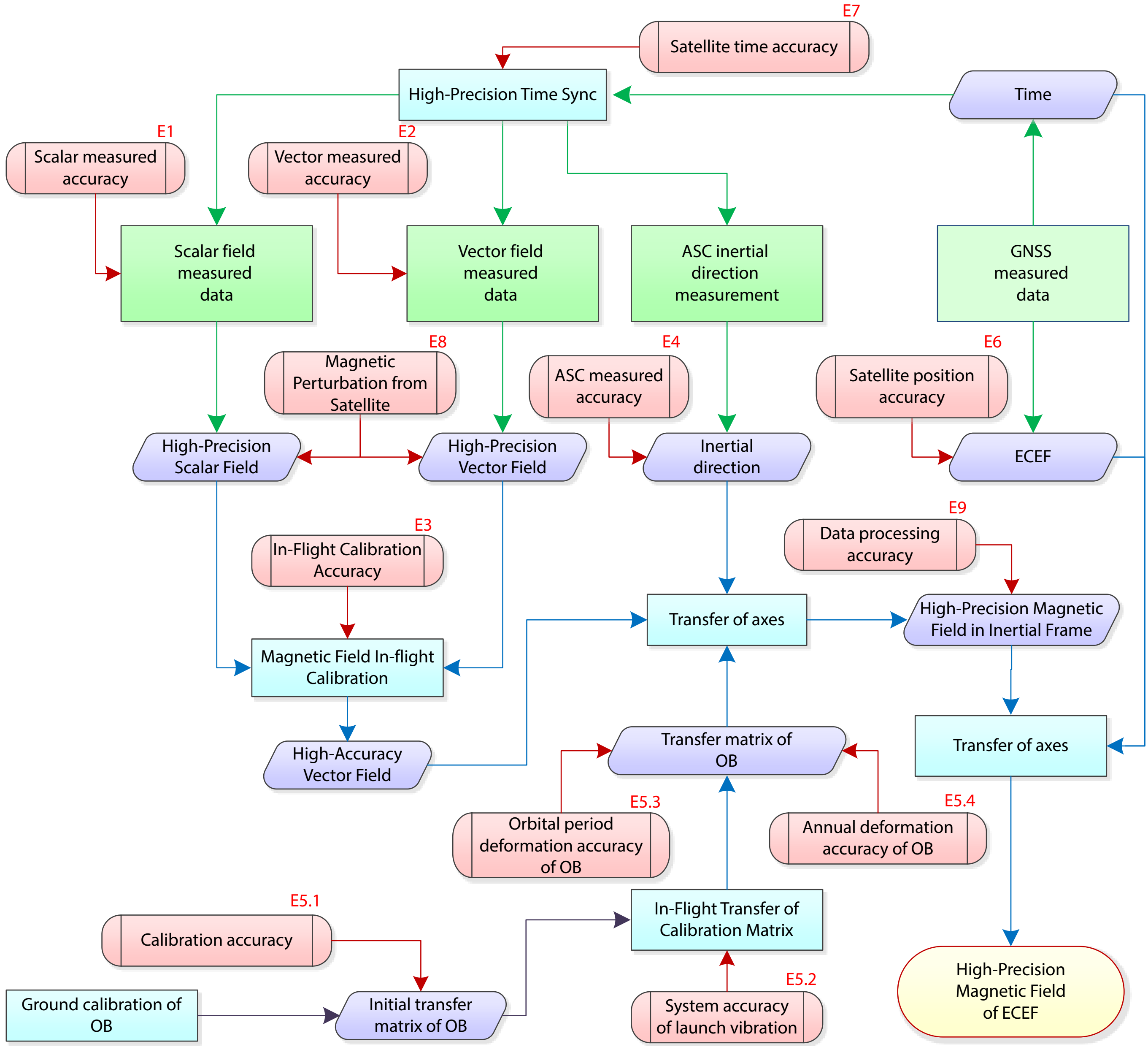

Figure 4. The full accuracy chain of high-precision magnetic field measurement. ASC, micro Advanced Stellar Compass; ECEF, Earth-centered, Earth-fixed coordinate system; OB, optical bench.

fore, controlling the deformation of the optical bench is one of the most critical technical challenges and focal points for the MSS-1A satellite. This design strategy was adopted for the MSS-1A satellite by building on the approach successfully implemented by the CHAMP and Swarm missions, which integrated magnetometers and star trackers onto the optical bench as primary payloads, thereby substantially improving the stability of the transfer matrix between the magnetometers and star sensors. The design integrates a nonmagnetic, high-precision thermal control system that combines multi-stage thermal insulation, directional heat dissipation from heat sources, and high-precision nonmagnetic temperature regulation, effectively resolving critical challenges in technologies, such as arc-second-level thermal stability control and nonmagnetic thermal management. These improvements markedly enhance the stability of the optical bench.

To address the high thermal stability requirements of the optical bench for the MSS-1A satellite, a measurement system based on

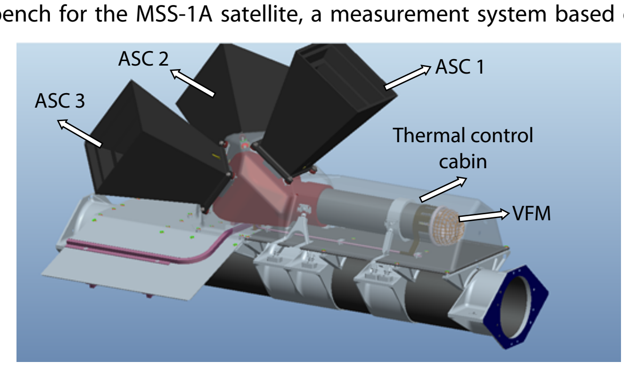

Figure 5. The MSS-1A optical bench. ASC, micro Advanced Stellar Compass; VFM, Vector Field Magnetometer.

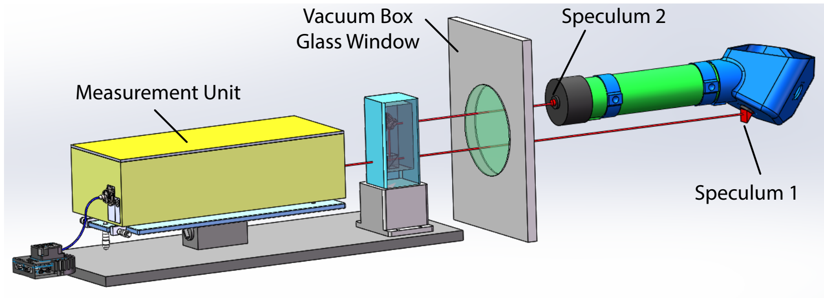

Figure 6. Ground-based laser measurement system.

the laser fiber autocalibration angle measurement method has been developed (see Figure 6), achieving a measurement accuracy of up to 0.25 arc seconds and a resolution of 0.1 arc seconds.

The thermal stability test of the optical bench was carried out under high- and low-temperature cycling conditions (e.g., Zhang H et al., 2023). The actual measurement data from the system were used to refine the thermal deformation simulation model. The results obtained for the thermal stability of the optical bench under in-flight temperature conditions are as follows: The thermal stability between the axes of the VFM body coordinate system and the ASC optical axis was better than 0.10 arc seconds (per orbit period)/2.6 arc seconds (per year period). The thermal stability of the ASC optical axis itself was better than 0.10 arc seconds (per orbit period)/0.81 arc seconds (per year period).

Compared with the thermal stability of the Swarm satellite's optical bench, the root mean square (RMS) value of the angular variation between the ASC optical axes of the MSS-1A satellite is a maximum of 0.46 arc seconds, which is approximately 82% lower than the corresponding value of 2.6 arc seconds for the Swarm satellite.

During the initial in-flight phase, the amplitude of temperature variation of the carbon-fiber boom in the thermal control cabin within the β-angle variation cycle and within a single orbit was significantly lower than the ground simulation results. The amplitude of temperature variation of the ASC bracket within the thermal control cabin within the β-angle variation cycle and within a single orbit was comparable to the ground simulation results. The amplitude of temperature variation of the kinematic legs, VFM probe, and ASC probe within the β-angle variation cycle was significantly lower than the ground simulation results, whereas the amplitude of temperature variation within a single orbit was comparable to the ground simulation results.

On the basis of the in-flight thermal environment characterization of the optical bench, the ground simulation temperature-field model was optimized to enhance its predictive fidelity (see Table 3, Figure 7). A representative subset of orbital thermal load cases was systematically analyzed to evaluate the thermal stability of the platform. As summarized in Table 3, the relative thermal stability between the VFM body coordinate axes and the ASC optical axis was measured at 0.1 arc second/orbit (1σ) and 0.86 arc second/year (1σ), whereas the interaxis stability among ASC optical axes remained below 0.07 arc second/orbit and 0.66 arc second/year. These in-orbit performance metrics exhibit close alignment with ground-based thermal stability simulations (deviation <5%), thereby experimentally validating that the optical bench complies with the deformation tolerance specifications of <1 arc second/orbit and <3 arc seconds/year.

Table 3. Initial in-flight temperature of the optical bench.[a]

Instrument	Average temperature in 2024 (°C)	Temperature variation in one day (°C)	Temperature variation in one cycle (°C)
VFM TOB33	From −4.25 to 5.328	≤0.74	≤0.14
ASC TOB34–TOB36	From −5.754 to 1.61	≤1.67	≤1.05

[a]TOB, Temperature of Optical Bench.

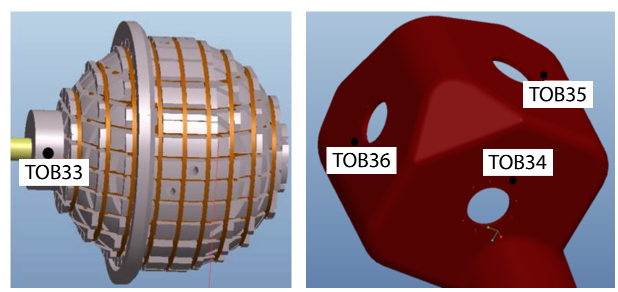

Figure 7. TOB (Temperature of Optical Bench) of the micro Advanced Stellar Compass (ASC) and Vector Field Magnetometer (VFM).

4.3 Calibration Transfer Matrix

Accurate calibration of the transfer matrix from the coordinate system of the VFM to that of the ASC is one of the crucial means for improving the accuracy of magnetic field measurement. The VFM and three ASCs are rigidly connected and mounted via the optical bench, based on experience from the Swarm satellite. The inertial-space orientation of the vector magnetic field can be precisely restored through a comprehensive and accurate calibration of the transfer matrix.

The basic principle formula for ground calibration is as follows:

$$\boldsymbol{B}_{\mathrm{NEC}} = \boldsymbol{M}_{\mathrm{NEC}\leftarrow\mathrm{WGS}}\boldsymbol{M}_{\mathrm{WGS}\leftarrow\mathrm{ECI}}\boldsymbol{M}_{\mathrm{ECI}\leftarrow\mathrm{ASC}}\boldsymbol{M}_{\mathrm{ASC}\leftarrow\mathrm{VFM}}\boldsymbol{B}_{\mathrm{VFM}}, \quad (1)$$

where $\boldsymbol{B}_{\mathrm{NEC}}$ is the Earth's vector field in the NEC (North–East–Center) coordinate system; $\boldsymbol{M}_{\mathrm{NEC}\leftarrow\mathrm{WGS}}$ is the transfer matrix from the WGS (World Geodetic System) coordinate system to the NEC coordinate system; $\boldsymbol{M}_{\mathrm{WGS}\leftarrow\mathrm{ECI}}$ is the transfer matrix from the ECI

(Earth-Centered Inertial) coordinate system to the WGS coordinate system; $\boldsymbol{M}_{ECI \leftarrow ASC}$ is the transfer matrix from the ASC coordinate system to the ECI coordinate system; $\boldsymbol{M}_{ASC \leftarrow VFM}$ is the transfer matrix from the VFM coordinate system to the ASC coordinate system; and $\boldsymbol{B}_{VFM}$ is the measured vector value of the VFM.

4.4 Magnetic Cleanliness Control

Controlling the satellite's overall residual magnetism and the residual magnetic field of soft magnetic materials inside the satellite after magnetization by external magnetic fields are key aspects of magnetic control. A comprehensive magnetic cleanliness control standard has been established according to these requirements that covers all levels, from materials, individual components, and subassemblies to the entire satellite. The magnetic cleanliness control design from the China Seismo-Electromagnetic Satellite (CSES) has been partially adjusted and redesigned to align with the mission characteristics of the MSS-1A satellite (e.g., Shen XH et al., 2018; Yuan SG et al., 2018). For the first time, a high-magnetic-cleanliness assembly process plan featuring nonmagnetic or low-magnetic tool materials and a thermal control lead routing method based on current reverse twisted and multi-layer circuit breaker layout has been proposed. This has led to a breakthrough in ultra-clean magnetic cleanliness control technology at the satellite system level, ultimately achieving the goal of keeping the satellite's magnetic disturbance below 0.2 nT.

For the first time in China, a ground measurement device for extremely weak residual magnetism has been developed. This device has the appearance of a bucket with a diameter of 800 mm (see Figure 8), which is used to screen materials and components in an extremely weak magnetic field environment. With this device, ground magnetic tests and calibration were carried out on the MSS-1A satellite. After testing, the overall magnetic cleanliness of the satellite was better than 0.105 nT, which is more than twice the magnetic cleanliness control level of 0.33 nT for the CSES.

4.5 Preliminary In-Orbit Testing

As China's first dedicated high-precision geomagnetic field survey satellite, the MSS-1A is required to achieve measurement accuracy for the three-component magnetic field and the total magnetic field strength of better than 0.5 nT. To meet this goal, the following design considerations have been adopted for the MSS-1A satellite:

Figure 8. Specific magnetic cleanliness measurement device.

(1) *Design development in collaboration with leading international institutions*: The satellite is equipped with state-of-the-art magnetic field exploration payloads through cooperation with leading international institutions in the field of magnetic measurement. The scalar magnetometer was developed by the Austrian Academy of Sciences, whereas the vector magnetometer was developed by the Technical University of Denmark.

(2) *Optical bench with low-deformation and nonmagnetic temperature control*: An optical bench with extremely low deformation and nonmagnetic temperature control is used to rigidly connect and install the vector magnetic field payload and the star tracker. An accurate transfer matrix is obtained through a ground-based integrated magnetic-optical calibration test to precisely restore the inertial-space orientation of the vector magnetic field.

(3) *Full-process magnetic cleanliness control*: Full-process magnetic cleanliness control is implemented for the MSS-1A satellite. In particular, a nearly "zero magnetic" design has been achieved for the boom and the optical bench close to the sensors to eliminate the satellite's own magnetic interference.

The implementation of high-precision magnetic field measurement accuracy has been analyzed based on the in-flight test results. The total combined accuracy for the three components of the magnetic field and the total magnetic field strength of the satellite are approximately 0.303 nT and 0.388 nT, respectively.

After the CDSM is locked in-flight, it continuously measures magnetic field data. The magnetic field of the MSS-1A satellite is mapped and compared with data from the CHAOS model at the same altitude, showing good overall agreement, as illustrated in Figure 9.

Figure 10 shows the scalar magnetic field distribution at 500 km altitude based on the CHAOS model. The scalar magnetic field measurements from the MSS-1A satellite and the Swarm satellite clearly show a very similar distribution when compared with the CHAOS model in terms of the mean value, variance, and distribution pattern.

The CHAOS-7 model is used as a standard to evaluate the data from MSS-1A and Swarm. Because of the strong external field interference in high-latitude regions, the Swarm data are more

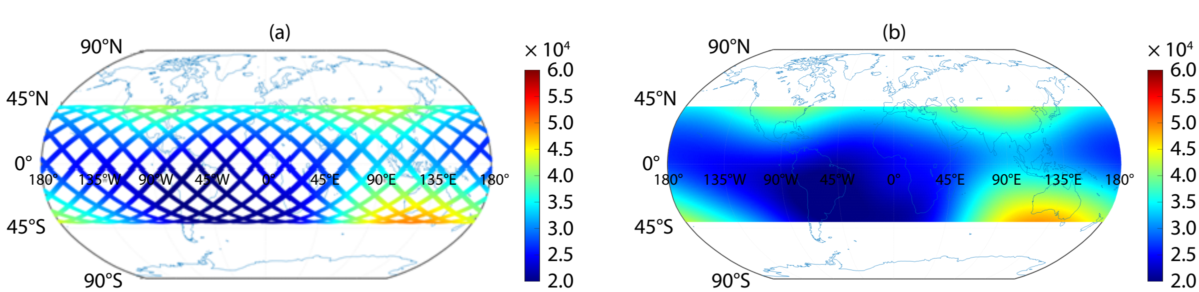

Figure 9. Comparison between MSS-1A data (a) and data from the CHAOS model (b).

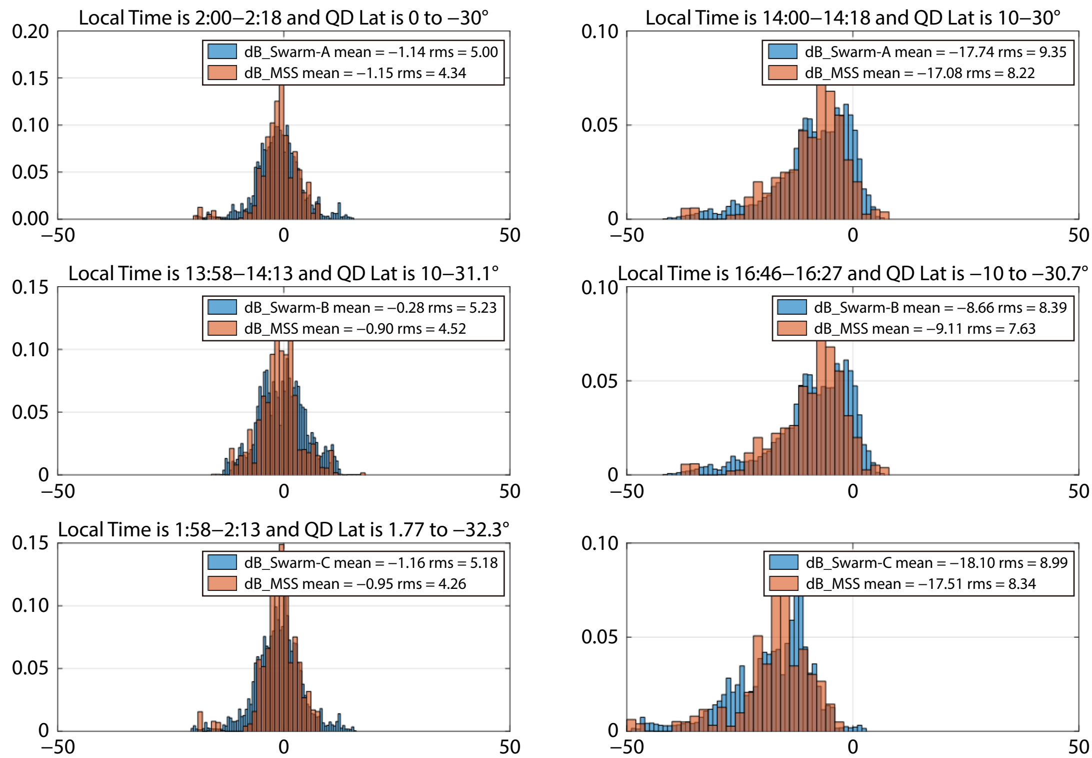

Figure 10. Comparison between MSS-1A and Swarm scalar data and results of the CHAOS model. QD Lat, quasi-dipole latitude; rms, root mean square.

substantially affected by interference in these areas. However, in low-latitude regions, especially in the same latitude areas as data from the MSS-1A satellite, the residuals of the vector data from the MSS-1A satellite (in orange, Figure 11) have the same distribution as those of the Swarm satellites (e.g., Jiang Y et al., 2024). The RMS deviations are shown in Table 4.

Table 4. The RMS (nT) of the differences.

Satellite	B_X	B_Y	B_Z
Swarm	9.48	15.95	7.65
MSS-1A	7.49	8.09	4.19

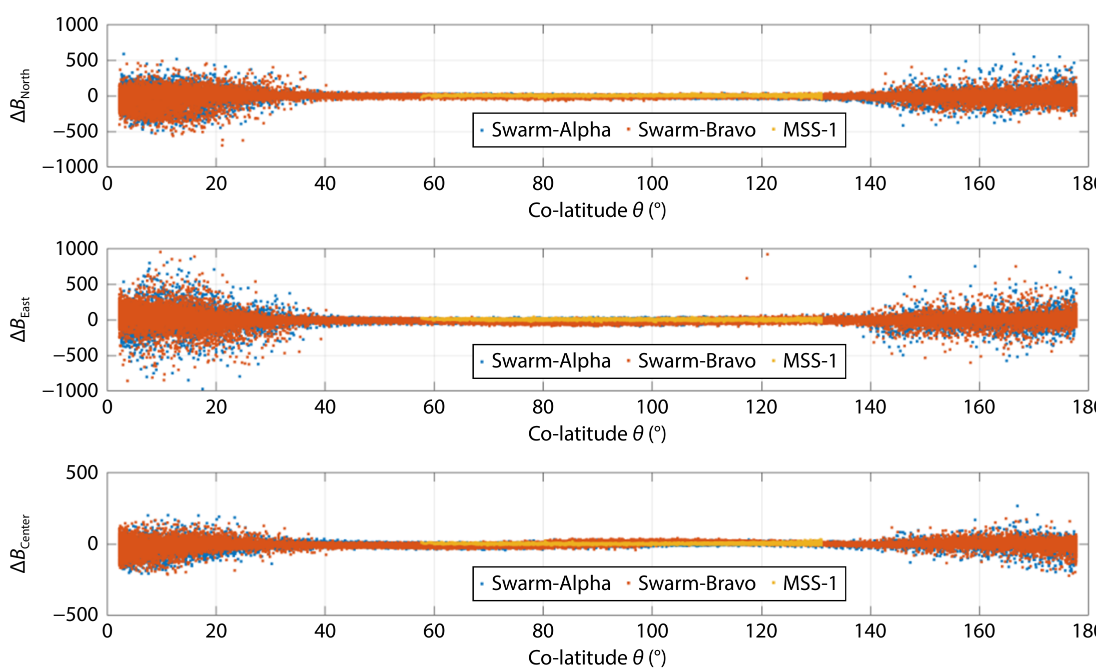

Figure 11. Comparison between MSS-1A and Swarm vector data and CHAOS model data.

Moreover, owing to the unique characteristics of its orbit, the MSS-1A satellite achieves all local time coverage in just 52 days — less than a quarter of the time required by Swarm (267 days). This enhanced temporal resolution presents new opportunities for investigating rapidly changing geomagnetic phenomena.

5. Conclusions

The MSS-1A has achieved in-flight measurement accuracy for both the three-axis magnetic field and total magnetic field intensity that is fully consistent with the ground test results. As China's first satellite dedicated to high-precision geomagnetic field detection, the MSS-1A uses the same high-precision magnetic payloads as the Swarm satellite, draws on the development experiences and lessons of the Swarm satellite, and integrates domestic advantages for optimization and innovation. Consequently, several important technological breakthroughs have been accomplished, including the development of a high-stability nonmagnetic optical bench, ultra-high magnetic cleanliness control at the satellite system level, and system-level ground calibration for high-accuracy vector magnetic field measurement in space. These innovations provide more accurate data and advanced technical means for future geomagnetic satellite missions, which helps promote the in-depth development of global geomagnetic field research. Their successful experiences also serve as valuable references for subsequent satellite missions, especially in aspects such as satellite design, data processing, and international cooperation. The successful development and operation of the satellite offer crucial data support for China in multiple fields, such as geomagnetic field research, space weather monitoring, geological exploration, and disaster early warning systems. Furthermore, these successes lay a solid foundation for the development of China's subsequent geomagnetic field exploration satellites.

Acknowledgments

We thank all the authors for their full assistance in providing the data and content related to this article.

References

Cheng, B. J., Zhou, B., Magnes, W., Lammegger, R., and Pollinger, A. (2018). High precision magnetometer for geomagnetic exploration onboard of the China Seismo-Electromagnetic Satellite. *Sci. China Technol. Sci.*, *61*, 659–668. https://doi.org/10.1007/s11431-018-9247-6

Feng, Y., An, Z. C., Sun, H., Mao, F. (2010). Geomagnetic survey satellites. *Progress in Geophysics*, *25*(6), 1947–1958. https://doi.org/10.3969/j.issn.1004-2903.2010.06.009

Friis-Christensen, E., Lühr, H., Hulot, G. (2006). Swarm: A constellation to study the Earth's magnetic field. *Earth Planets and Space*, *58*(4), 351–358. https://doi.org/10.1186/BF03351933

Jiang, Y., Finlay, C. C., Olsen, N., Tøffner-Clausen, L., Yan, Q., and Zhang, K. (2024). Macau Scientific Satellite-1 Initial Magnetic Field Model. *Geophysical Research Letters*, *51*(22), e2024GL112305. https://doi.org/10.1029/2024gl112305

Liu, J. H., Wen, Q., and Wang, Z. K. (2024). Frontiers in geomagnetic satellite measurement technology. *Space International (in Chinese)*, (1), 56–63.

Meng, L. F., Xu, C. Q., Xiao, Q., Liu, C. B., Geng, X. L., Chen, D. X., Yi, Z., and Zhang, T. L. (2024). A high-precision system level calibration method for spaceborne magnetometers. *Chinese Space Science and Technology (in Chinese)*, *44*(3), l74–179. https://doi.org/10.16708/j.cnki.1000-758X.2024.0051

Ness, N. F., Behannon, K. W., Lepping, R. P., Schatten, K. H. (1971). Use of two magnetometers for magnetic field measurements on a spacecraft. *J. Geophys. Res.: Space Phys., 76*(16), 3564–3573. https://doi.org/10.1029/JA076i016p03564

Shen, X. H., Zhang, X. M., Yuan, S. G., Wang, L. W.,Cao, J. B., Huang, J. P., Zhu, X. H., Piergiorgio, P., and Dai, J. P. (2018). The state-of-the-art of the China Seismo-Electromagnetic Satellite mission. *Sci. China Technol. Sci.*, *61*(5), 634–642. https://doi.org/10.1007/s11431-018-9242-0

Yuan, S. G., Zhu, X. H., and Huang, J. P. (2018). System design and key technology of China Seismo-Electromagnetic Satellite. *J. Remote Sens.*, *22*(Sup), 32–38. https://doi.org/10.11834/jrs.20188177

Zhang, H., Liu, Z. Q., Yu, C. Y., Luo, W. B., and Yuan, D. (2023). Thermal stability design and verification of optical bench structure of geomagnetic survey satellite. *Journal of Astronautics*, *44*(10), 1604–1612. https://doi.org/10.3873/j.issn.1000-1328.2023.10.013

Zhang, K. (2021). A high-precision and highly-elliptical-orbit geomagnetic constellation. *Presentation at 11th Swarm Data Quality Meeting*, *Athens*, Greece.

Zhang, K. (2023). A novel geomagnetic satellite constellation: Science and applications. *Earth Planet. Phys.*, *7*(1), 4–21. https://doi.org/10.26464/epp2023019